symmetry

MDPI

Article

Oligomeric Symmetry of Purine Nucleoside Phosphorylases

Boris Gomaz and Zoran Štefanić *

Division of Physical Chemistry, Ruđer Bošković Institute, Bijenička cesta 54, 10000 Zagreb, Croatia; boris.gomaz@irb.hr

* Correspondence: zoran.stefanic@irb.hr; Tel.: +385-1-4571405

Abstract: Many enzymes are composed of several identical subunits, which are arranged in a regular fashion and usually comply with some definite symmetry. This symmetry may be approximate or exact and may or may not coincide with the symmetry of crystallographic packing. Purine nucleoside phosphorylases (PNP) are a class of oligomeric enzymes that show an interesting interplay between their internal symmetry and the symmetry of their crystal packings. There are two main classes of this enzyme: trimeric PNPs, or "low-molecular-mass" proteins, which are found mostly in eukaryotic organisms, and hexameric PNPs, or "high-molecular-mass" proteins, which are found mostly in prokaryotic organisms. Interestingly, these two enzyme classes share only 20–30% sequence identity, but the overall fold of the single monomer is similar, yet this monomeric building block results in a different quaternary structure. To investigate this interplay of symmetry in this class of enzymes, a comprehensive database of all PNPs is constructed, containing their local symmetries and interface information.

Keywords: oligomeric enzymes; purine nucleoside phosphorylases; crystal symmetry

1. Introduction

Symmetry and oligomerization are ubiquitous phenomena in proteins and are closely related to protein stability and function [1]. A large proportion of the structures deposited in the PDB [2,3] display some kind of symmetric arrangement. Considering all proteins deposited in the PDB, 40.4% are symmetric, with 31.5% displaying cyclic symmetry and 7.3% showing dihedral symmetry. Oligomeric proteins, which consist of several identical subunits (chains), are often arranged in a regular fashion, following a point-group symmetry. This is often referred to as a protein-quaternary structure. If we take into account only the oligomeric proteins, the proportions of symmetric arrangements are much higher. Depending on whether the subunits of oligomeric proteins are the same or different, they are referred to as homomeric or heteromeric, respectively. The quaternary organization of proteins is increasingly studied [4–6], as the improper organization of protein subunits can lead to malfunction, poor allosteric regulation (and modulation), or both. The stability of proteins depends on the interfaces and the interactions that occur between amino acids on the interfaces. Generally, the larger the interface area between the two subunits, the stronger the binding force. The vast majority of protein structures are determined by X-ray crystallography (around 89% of all the structures in the PDB). In crystal packing, the symmetric arrangement of oligomeric proteins is combined with the symmetry operations of the crystal lattice. Sometimes, the crystal symmetry coincides exactly with the symmetry present in a protein oligomer, making only part of the oligomer symmetrically independent. There are many ways in which the symmetry of the space group may be exploited [7]. Although the crystal packing interactions of monomers are generally weaker and smaller in size, they may become comparable to the interactions between monomers in their biological state. This may sometimes complicate the determination of the native oligomeric state of the protein [8]. Several approaches have been used in the past to determine the oligomeric

check for updates

Citation: Gomaz, B.; Štefanić, Z. Oligomeric Symmetry of Purine Nucleoside Phosphorylases. *Symmetry* **2024**, *16*, 124. https://doi.org/10.3390/sym16010124

Academic Editor: Arkadiusz Chworos

Received: 28 December 2023
Revised: 16 January 2024
Accepted: 17 January 2024
Published: 19 January 2024

state from the crystal structures. However, none of the proposed methods are fully accurate, and there are still cases where this determination is not straightforward [9–11].

A family of oligomeric enzymes that exhibit an interesting interplay between their internal symmetry and crystal symmetry are purine nucleoside phosphorylases (PNPs) [12,13]. There are two main classes of this enzyme: trimeric PNPs, or "low-molecular-mass" proteins, found mostly in eukaryotic organisms, and hexameric PNPs, or "high-molecular-mass" proteins, found mostly in prokaryotic organisms [12,14,15]. Both forms take the same substrate, guanine and hypoxanthine (2′-deoxy) ribonucleoside. However, there are cases where hexameric and trimeric PNPs can also process adenine (2′-deoxy) ribonucleoside. PNPs belong to the family of glycosyltransferases and are found in all organisms, from bacteria to humans. PNPs catalyze a reversible ribosyl reaction, transferring from the (deoxy)purine nucleoside to orthophosphate [16,17]. These enzymes play a key role in the salvage pathway, an alternative way of synthesizing nitrogenous bases and nucleosides by salvaging fragments of DNA/RNA. In organisms that completely lack the de novo pathway of purine synthesis, this purine salvage pathway is the only way they acquire the essential building blocks for DNA synthesis [18]. As a result, this makes the PNPs in certain bacteria, such as *Helicobacter pylori*, a very attractive drug target [19].

Trimeric PNPs are composed of three identical chains, with an average length of 290 amino acids. These three chains are arranged in cyclic C_3 symmetry, where three monomers form a three-membered circle (or, equivalently, an equilateral triangle). On the other hand, hexameric PNPs are composed of six identical chains with an average length of 244 amino acids. Each chain is connected with two-fold symmetry to a neighboring monomer, forming a symmetric dimer. Then, three such dimers are rotated by a three-fold symmetry perpendicular to the two-fold axis, completing the full hexamer with dihedral D_3 symmetry (Figure 1). Overall, this results in trimeric PNPs possessing point group 3 symmetry, while hexameric PNPs possess 32-point group symmetry. Although trimeric and hexameric PNPs share only 20–30% sequence similarity, the overall fold of their single monomers is remarkably similar (Figure 2) [20]. On the other hand, despite the shape similarity of the monomeric building blocks, they assemble into different quaternary structures. It is known that the oligomerization of these enzymes is required for their function, despite the fact that, in principle, even single monomers could conduct catalysis [21,22]. This relates to the increased structural stability of the oligomeric form and the allosteric regulation between the subunits in the oligomers [23]. Previously, in our work on PNPs, we discovered some peculiar features of active site conformations in some crystal structures [14]. In order to investigate the symmetry relationships within PNPs and their connection with the crystallographic symmetry appearing in their crystal structures, we classified the possible symmetry arrangements in this study.

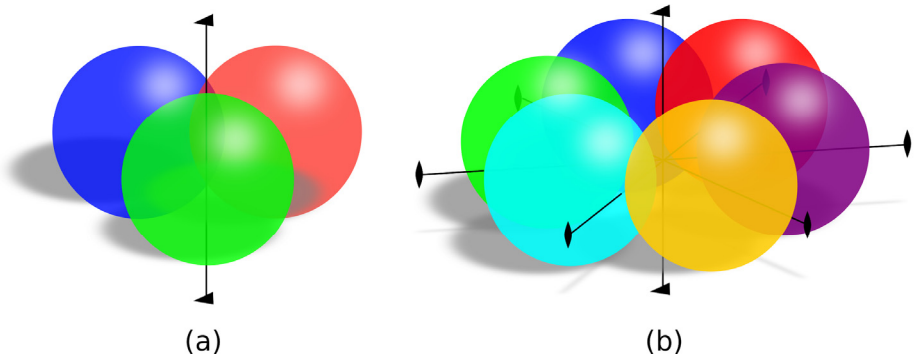

Figure 1. Schematic representation of two prevalent symmetry arrangements found in the PNP structures, with each monomer (chain) depicted as one colored sphere; (**a**) cyclic three-fold symmetry is characteristic of trimeric PNPs, and the point group is noted as 3 (or C_3 in Schoenflies notation); (**b**) dihedral symmetry (point group 32 or D_3 in Schoenflies notation), where the three-fold axis has three two-fold axes perpendicular, is characteristic of hexameric PNPs.

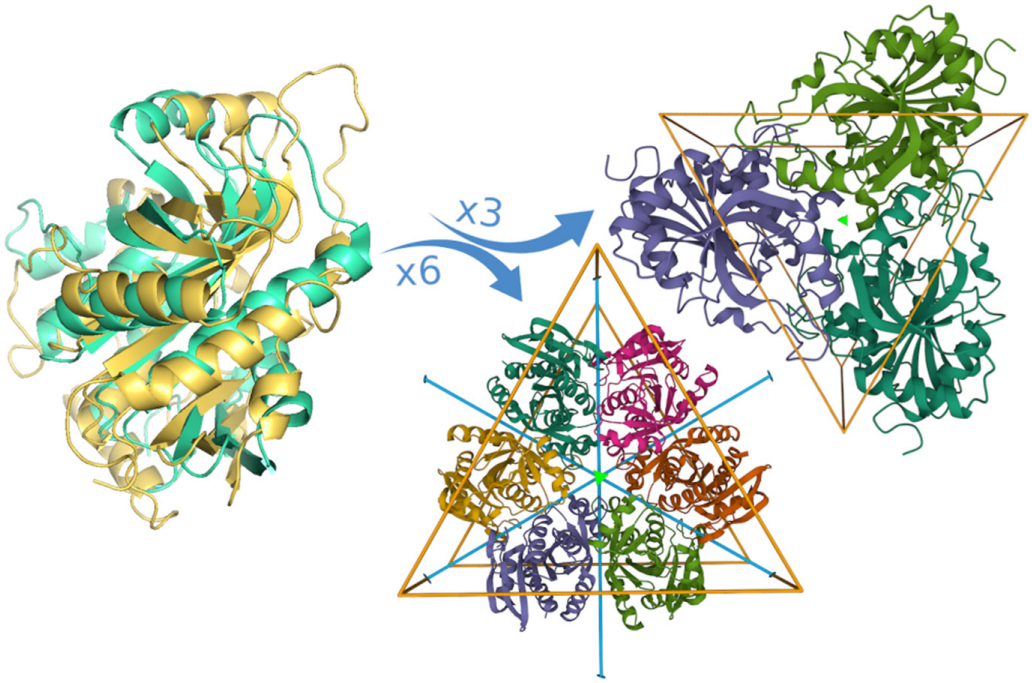

Figure 2. The overlap between one chain of trimeric PNP (gold) and hexameric PNP (teal) shows excellent 3D overlap and high fold conservation despite a rather low sequence similarity of only 20–30%. However, these two similar monomeric subunits assemble to form quite different quaternary structures: trimeric and hexameric PNPs, shown on the right.

2. Materials and Methods

In order to investigate the oligomerization and allosteric communication between the monomeric subunits of PNPs, a specially designed database of the structural data from 224 PNPs was constructed. The data on most aspects treated in this manuscript are also available on the web page (https://alokomp.irb.hr/, accessed on 27 December 2023). In the backend of the web page, there is a comprehensive database of all the structural data of PNPs derived from the PDB, which is additionally enriched with the relationships between structural data and sequence data. It features multiple sequence alignments of all PNPs [24], all-to-all chain alignments, 3D structural alignments [25], and data derived from molecular dynamics simulations on the selected PNPs. The sequence alignment was performed using Biopython [26], a set of Python tools for computational molecular biology, and a specific tool named Clustal Omega [24]. The web version of the multiple sequence alignments (https://alokomp.irb.hr/d3/ accessed on 27 December 2023) was visualized using the D3.js library [27], which is a JavaScript library for manipulating documents based on data. The multiple-sequence alignment in Figure S1 was created using PyMSAviz [28]. The structural alignment of all chains was calculated using the GESAMT tool [25], which is a supported program in the CCP4 suite (version 8.0.010) [29], software for macromolecular X-ray crystallography. The resulting data from the chain-to-chain alignment was processed using various Python libraries, and the heatmap figures were created by Seaborn [30]. For calculating the contact of residues and symmetry operations between the monomers, the CCTBX library was used [31]. The interface and contact analysis were created with the data drawn from the EPPIC web server at https://www.eppic-web.org (accessed on 27 December 2023) [32]. Using the REST API from https://www.eppic-web.org/rest/ (accessed on 27 December 2023), the data of all 224 PNPs contained in the database were programmatically downloaded and inserted into the database in a suitable form. The figures of simplified crystal packings were produced with the Pymol program (version 2.3.0) [33].

3. Results

3.1. Structural Alignment

To compare the individual differences between the different chains, a comprehensive database of the structural alignments was constructed. Each chain from the pool of structures determined by X-ray crystallography overlapped with every other chain using the GESAMT [25]. This resulted in the pairwise alignment of all the chains, with 176,715 alignments in total (with almost 37 million individual matches between residues, each characterized by similarity in scores and distance). Each alignment is characterized by several measures of fitness: Q-score, RMSD, percent of sequence identity, and number of aligned residues [25]. All alignments are visible on the page (https://alokomp.irb.hr/alignments/list/ accessed on 27 December 2023). We used the Q-score to produce an all-to-all clustering of PNP chains. This leads to the clear separation of all PNPs into two large classes, corresponding to hexamers and trimers (Figure 3). There is also an additional component that corresponds to a very small proportion of PNPs, which are neither hexameric nor trimeric. These other structures are either monomeric (6) or dimeric (4). Although they share some similarity on a monomer level, they are not interesting from a symmetry standpoint.

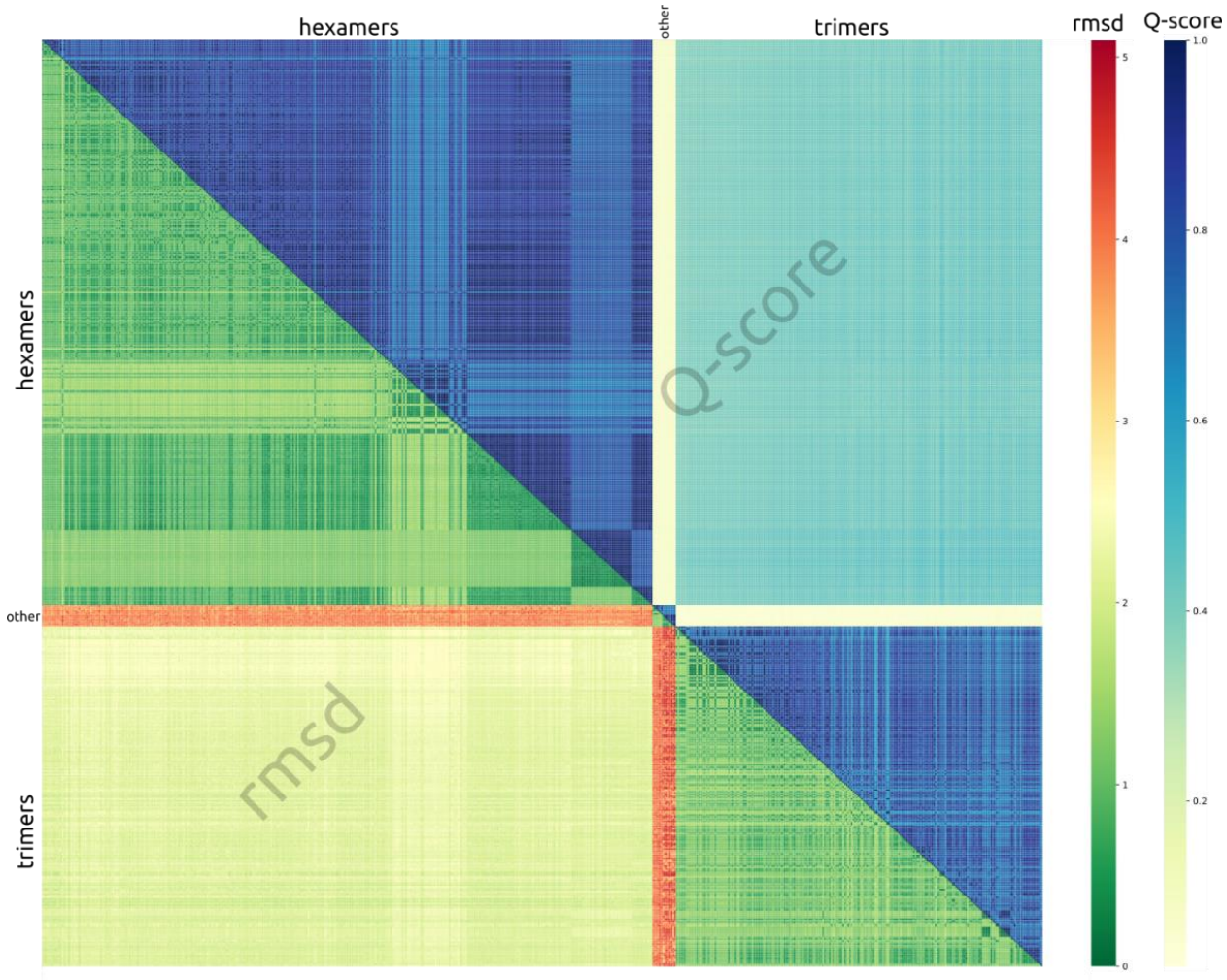

Figure 3. Q-score and rmsd distributions between the chains of all PNPs. A very clear separation between the hexamers and trimers is visible. In the middle, there is a small portion of PNPs, which are neither hexamers nor trimers and have a very poor Q-score below 0.15 and rmsd over 4 Å. The chains from the hexamers and trimers have an average Q-score of 0.4–0.6 between themselves (upper right corner) and rmsd between 2–3 Å.

3.2. Multiple Sequence Alignment

For any sort of comparison between the different structures, one common point of reference is needed to know which amino acids in one structure correspond to which other amino acids in some other structure. A natural way of finding such a common reference is by using multiple sequence alignments. Thus, all-to-all multiple sequence alignments were performed with chains from all PNPs (Figure S1). This allowed the unique assignment of positions for every amino acid in every chain, which correspond to each other. The overall length of the multiple sequence alignment is 405 positions, and there are 610 unique chains from all PNPs. Interestingly, the most conserved amino acid is Gly at position 133, and it is conserved in 100% of the cases. Unsurprisingly, this amino acid is situated in the active site, in the beta sheet region immediately below the purine aromatic ring binding pocket. Any larger amino acid would interfere with substrate binding [14]. The next most conserved amino acid is also Gly at position 42, corresponding to the Gly that binds the phosphate molecule deep in the active site, which is conserved in 97.7% of the PNPs. Perhaps unexpectedly, the third most conserved amino acid at position 88 is also Gly (at 94.3% conservation). However, this one is situated at a hairpin loop on the periphery of the monomer on the surface of the protein, with no obvious reasons for such a high degree of conservation. The only remaining amino acid that is conserved more than 90% is Met at position 250 (at 93%), which also takes part of the hydrophobic pocket for the purine binding pocket in the immediate vicinity of the substrate.

3.3. Distribution of Space Groups

The distribution of PNPs across the different space groups does not follow the general distribution of other proteins in the PDB. It can be noted that the space groups that contain either the three-fold or two-fold axis, or both, are present in a much higher proportion than in the general distribution (Figure 4). The two space groups with the highest number of structures are $P2_12_12_1$ and $P2_13$, with 43 structures each. The space group $P2_12_12_1$ is the most common space group in the PDB, with over 21% of the structures crystallizing in it. This explains the high number of PNPs that crystallize in this space group. This is in sharp contrast with the second-most popular space group, $P2_13$, with the same number of PNPs but a general abundance of only 0.44%. This space group has a three-fold axis. Next in line is the trigonal space group $R32$ (33 structures), with a general percentage of 1.2%. This space group contains the positions with site symmetry 32 that match exactly the point group symmetry of hexameric PNPs. Then comes the hexameric $P6_122$, with 24 structures and featuring several two-fold axes. Further down the list, there are other such space groups that have a much higher number of structures than would be expected if they followed the general distribution in the PDB ($P6_322$ with 14 structures, $P321$ with 7 structures, $R3$ with 5, and so on). All of them contain the symmetry of PNPs, as they contain the sites with the site symmetry, which is the subgroup of point group 32 and the full symmetry of hexameric PNPs, or point group 3 as the full symmetry of trimeric PNPs.

The reason for the preference of PNPs towards higher-symmetry space groups, which contain their own local symmetry, must be linked with the tendency to have only part of their oligomeric structure in the asymmetric unit of the crystal. The question then arises: how often in the crystal structures that crystallize in the space groups that contain the two-fold, three-fold, or both axes do these axes coincide with the non-crystallographic symmetry of the PNPs? In other words, how many trimers have one monomer in the asymmetric unit, or how many hexamers have one, two, or three monomers in the asymmetric unit? The results of this analysis are summarized in Table 1. In the case of 98 hexameric structures, there are 68 that contain either a three-fold or two-fold axis, or both. In the crystal structures that contain both axes, this symmetry is used by the hexamers in 77.4% of the cases (24 out of 31). This means that the point group symmetry of the hexamer is fully aligned with the crystallographic symmetry. In other words, the center of the hexamer coincides with the points with site symmetry 32 in their corresponding space groups. In the case of 37 crystal structures that contain only the two-fold axis, it is used in 33 cases (89.2% of the cases).

Also, there are no hexamers that crystallize in the space groups that contain three-fold symmetry but do not contain two-fold symmetry. The situation is quite the opposite for trimers. Since one trimer does not contain two-fold symmetry, this means that only in the space group, which contains three-fold symmetry, can there be an overlap between point group symmetry and crystal symmetry. But, then it occurs in 100% of the cases (78 out of 78), similar to point group 32 in the case of the hexamers. This means that the maximal point group symmetry of the hexamers (point group 32) and trimers (point group 3) is always fully satisfied if the space group contains the sites with that symmetry.

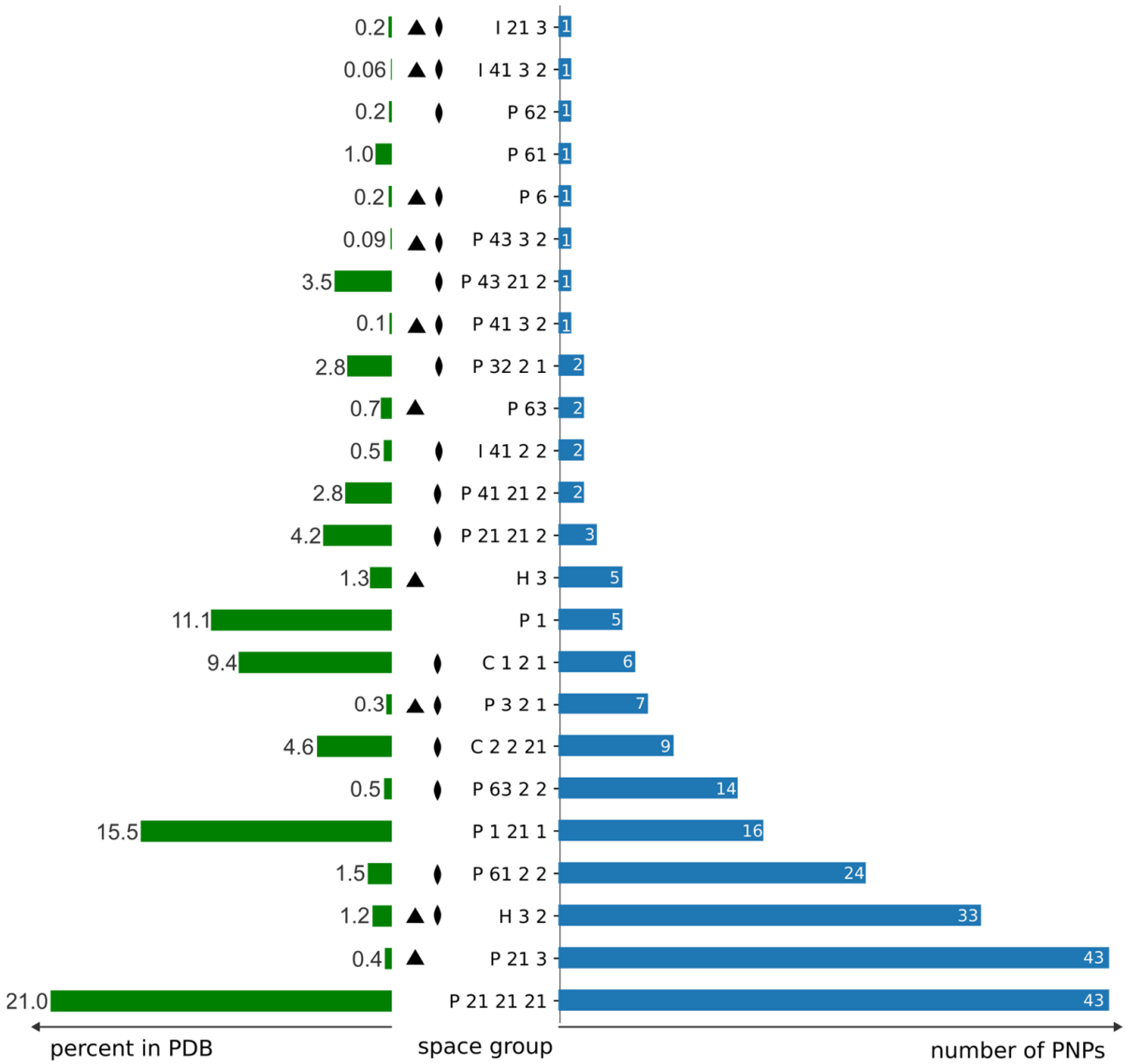

Figure 4. The distribution of the number of structures of PNPs across their space groups. In blue, the counts of structures in a particular space group are given. In green is the percentage of that particular space group across the entire PDB archive. It can be noted that PNPs are very prone to crystallizing in the higher symmetry groups, which are generally lower in number in the PDB, if they contain a three-fold and/or two-fold axis (denoted by their crystallographic symbols in black). Among the four most common space groups ($P2_12_12_1$, $P2_1$, $P1$, and $C2$), there is an unusually high proportion of rare high-symmetry groups with a general abundance below 1.5% ($P2_13$, $R32$, $P6_122$, $P6_322$, $P321$, and $R3$).

Table 1. The agreement between crystallographic symmetry and point group symmetry in the crystal structures of PNPs. Each cell shows two numbers: the first number shows how many cases of crystallographic symmetry coincide with the point group symmetry of the hexamers and trimers, and the second number is the total number of space groups that contain that symmetry.

Symmetry	Hexamers	Trimers	Others
only two-fold (point group 2)	33/37 (89.2%)	0/11 (0%)	0/2
only three-fold (point group 3)	0/0	50/50 (100%)	0
both (point group 32)	24/31 (77.4%)	28/28 (100%)	0
no two-fold or three-fold symmetry	0/30	0/27	11

Various possible arrangements displayed in the crystal structures of PNPs, with respect to space group symmetry, are summarized in Figure 5. Overall, there is a clear bias of both hexamers and trimers towards space groups that contain either two or three axes or both (most of the structures are roughly in the right three quarters of Figure 5). Also, it is apparent that any given space group symmetry can be utilized in multiple ways. For example, in hexameric structures that crystallize in space groups that contain points of site symmetry 32 (trigonal *P*321, *R*32; hexagonal $P6_322$ and cubic $I4_132$ and $P4_132$), there are three different arrangements: (a) most hexamers in this group exploit full symmetry, i.e., their centers coincide with points of 32 site symmetry; (b) there are some which use only the three-fold axes but not the two-fold, and therefore have two independent monomers in the asymmetric unit, and (c) there is one structure (PDB code 4m7w) which combines the (a) and (b) options and features one hexamer which utilizes full symmetry, and the other independent hexamer which uses only the three-fold axis (therefore three chains in the asymmetric unit) in the same crystal packing. A similar peculiar instance occurs in a trimeric structure with PDB code 4ns1, where one trimer uses the three-fold axis, but there is an additional trimer that does not have any exact symmetry, thus giving a structure with four chains in the asymmetric unit. One would maybe expect to find more space groups with hexagonal symmetry (six-fold axis) in the hexameric PNPs; however, there is only one group. The reason for this is that the hexamers possess dihedral 32-point group symmetry, not cyclic point group symmetry 6. Therefore, there is only one structure in the space group *P*6 (3mb8) that utilizes the three-fold symmetry also present in that space group. The number of chains in the asymmetric unit of hexamers ranges from 1 all the way up to 18 in the structure 3ooh, which has as many as three hexamers in the asymmetric unit. In trimers, this number ranges from one to at most six, i.e., two trimers in the asymmetric unit.

3.4. Crystal Packing Similarities

Crystal packings within the same space groups show an exceptional degree of analogy (the full list is available at https://alokomp.irb.hr/symmetry/gallery/ accessed on 27 December 2023). This is apparent in the simplified views of the crystal packings, where each monomeric subunit is represented by a sphere centered at the chain's center of mass (Figure 6). This applies to the hexamers and trimers. Some arrangements are similar in different space groups, such as the honeycomb structures of the hexamers in space groups *P*321, *R*32, and $P6_322$.

3.5. Contacts between Subunits

One significant difference between the hexameric and trimeric PNPs is the nature of the interfaces dictated by their symmetry [8]. Specifically, since the trimers have only cyclic three-fold symmetry, they can only have heterologous interfaces [34]. In contrast, all the interfaces between the monomers in the hexamers are isologous because they are operated by a two-fold axis. In hexamers, there are two different kinds of these isologous interfaces: intra-dimer and inter-dimer interfaces. This means that, in principle, the amino acids that participate in biological interfaces in the hexamers will be symmetric

with respect to the interchange of chain labels in the hexamers; however, this will not be true for trimers. To characterize all the interfaces formed in the crystal structures of PNPs, we used the Evolutionary Protein–Protein Interface Classifier (EPPIC) [32] web server. This method classifies the interfaces as biological and crystal contacts and gives an estimate of confidence in classification. The residue in each monomer can be part of several interfaces. It is interesting to look at how the amino acids involved in interfaces are distributed against positions in the multiple sequence alignment. This distribution is shown in Figure 7. It allows for comparison between these distributions—between the hexamers and trimers—because their amino acids are aligned. It is shown that the amino acids found on the interfaces are concentrated in several regions (marked I–IV in Figure 6), which are approximately aligned between the hexamers and trimers. This is expected since the evolutionary conservation, which is generally reflected in the multiple sequence alignment, is higher at the interfaces. On the other hand, if these regions are found in approximately the same places in the hexamers and trimers, this is in accordance with the similar overall shape of their building blocks (chains) between the hexamers and trimers (Figure 2) and their participation in the interfaces. Despite the evolutionary divergence of hexameric and trimeric PNPs, which leaves them at only 20–30% sequence similarity, the overall shape and the interfaces remain similar.

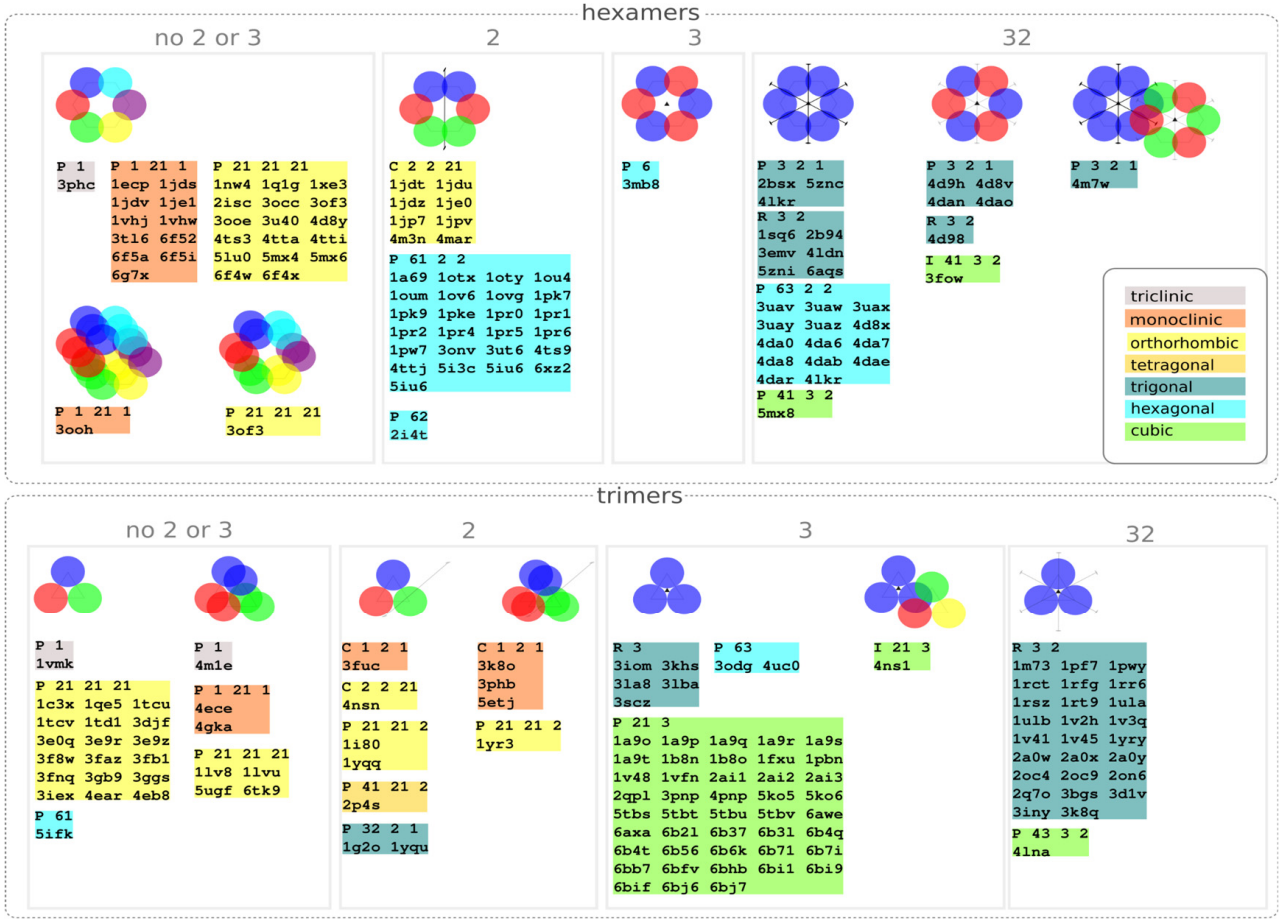

Figure 5. The types of arrangements of monomeric subunits (chains) of the hexameric and trimeric PNPs, with respect to the symmetry elements in the space group. Each box has a title with the symmetry that some sites may possess in the space groups given in that box. Inside each box, the structures (indicated by their PDB code) are grouped by their space group and colored by their crystal system.

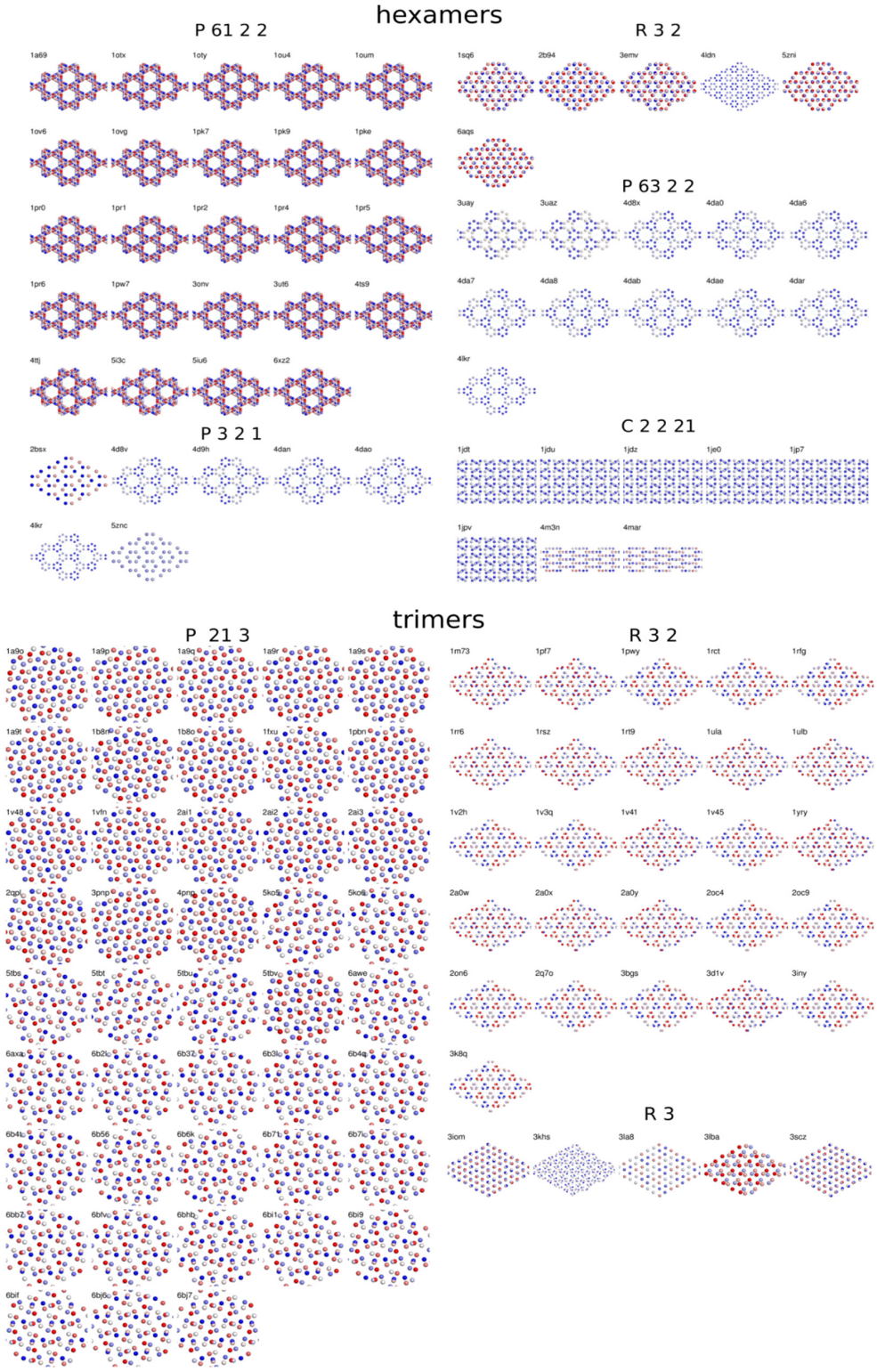

Figure 6. Simplified representation of the crystal structures of the hexameric PNPs in the most common space groups. Each sphere represents one monomer, and the projections are along the symmetry axis. The spheres are colored according to their distance from the plane of projection, from blue, which is—the closest to the plane of projection, to red, which is the farthest. It shows that the packings in the same space group are highly isomorphic. There are a few exceptions (e.g., PDB code 4ldn in the space group *R*32 and PDB codes 4m3n and 4mar in $C222_1$) that show that even in the same space group, utilizing the full 32-point group symmetry, the packing can be realized in multiple ways.

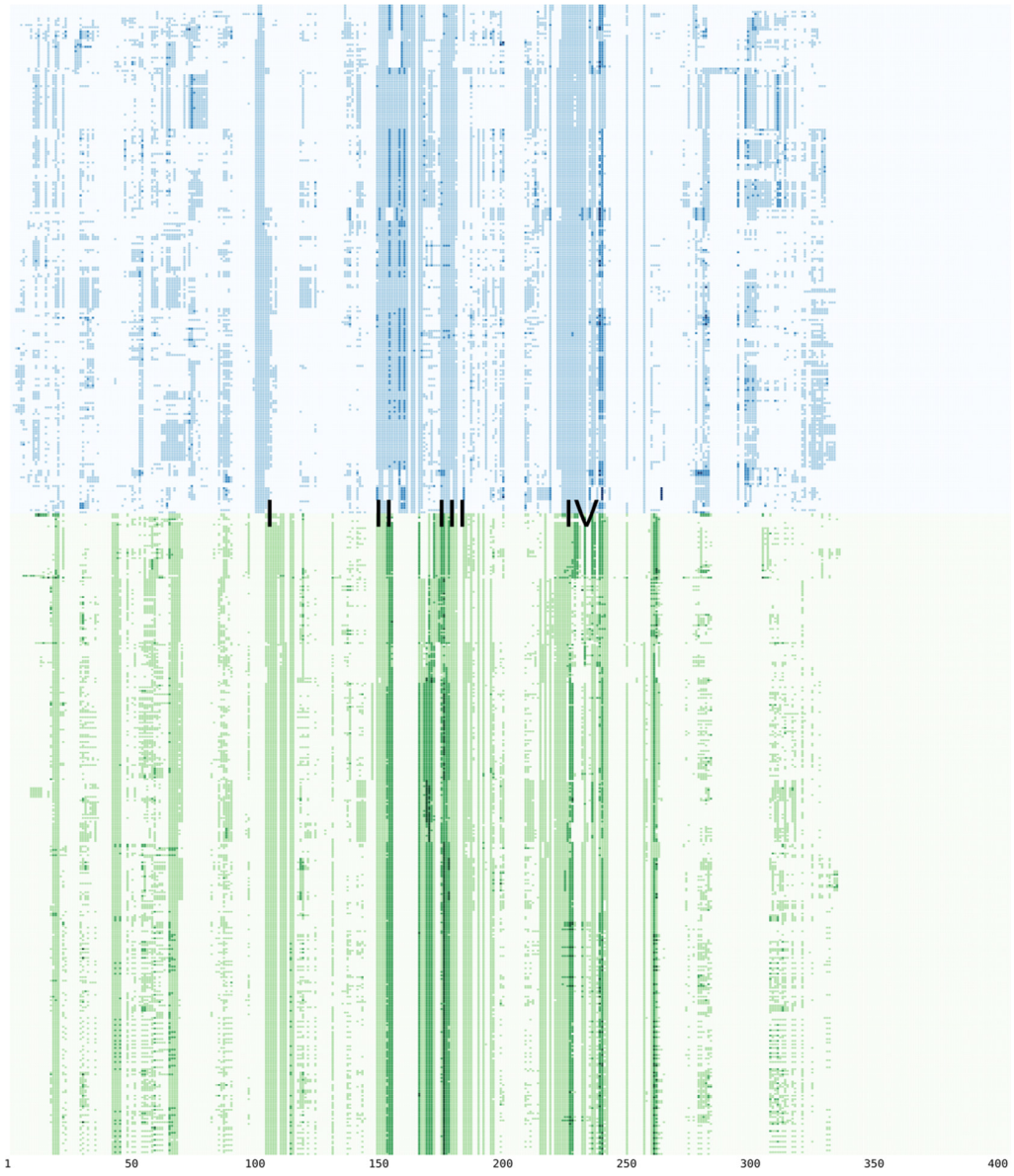

Figure 7. The heatmap distribution of the number of interface contacts between the different chains in the trimers (blue) and hexamers (green). On the horizontal axis are the positions of the multiple sequence alignment of all PNPs (from 1 to 405). Each horizontal row represents one chain of one PNP (labels are omitted for clarity). Each square dot represents one amino acid, colored by the number of different interfaces that it is part of. It can be noted that the regions where these interface contacts take place are approximately situated in the same position (in the regions denoted I–IV) and conserved throughout the PNPs.

4. Discussion

PNPs have evolved from the hexameric form in lower organisms to the trimeric form in higher organisms. Along the way, they have kept their original function despite a substantial change in quaternary structure and their primary sequence. It is yet another example of evolutionary function preservation. From the individual chain alignments, a very clear grouping of PNPs is visible, and there is very little variation within these groups (Figure 3). In addition, the scores between these groups are very consistent, indicating rather good fold conservation within each species, although the source organisms of various PNPs may vary substantially.

The local symmetry of PNPs strongly influences the symmetries realized in their crystal structures, radically altering the distribution pattern of observed space groups (Figure 4). This favors the groups that contain sites with symmetry 3 or 32. We have seen that, in the majority of the cases, the present crystallographic symmetry is fully exploited, meaning that the crystallographic axes of symmetry coincide with the axes of the point group symmetries of the hexamers and trimers. In the case of trimers, this is always fulfilled. This bias towards symmetries that contain favorable point group symmetries is superimposed on the general preference of proteins towards space groups, so that the most common space group in all proteins ($P2_12_12_1$) is still the most common in PNPs, but with the high-symmetry cubic space group, $P2_13$, having the same number of structures, and two rare space groups immediately following ($R32$ and $P6_122$). The preference for space groups that closely accommodate the symmetry of individual building blocks is an expected feature. This would likely be observed in other symmetric proteins. Nevertheless, it is remarkable and instructive to see such a high degree of agreement between local and space group symmetry.

Supplementary Materials: The following supporting information can be downloaded at: https://www.mdpi.com/article/10.3390/sym16010124/s1. Figure S1: Multiple sequence alignment of all PNP chains.

Author Contributions: Conceptualization, Z.Š. and B.G.; software, Z.Š. and B.G.; writing—original draft preparation, Z.Š. and B.G.; funding acquisition, Z.Š. All authors have read and agreed to the published version of the manuscript.

Funding: This research was funded by the Croatian Science Foundation, grant number IP-2019-04-6764.

Data Availability Statement: The data supporting the published results are available at the web page of the ALOKOMP project: https://alokomp.irb.hr/ accessed on 27 December 2023. The initial concept of the publication was presented at the 28th Croatian-Slovenian Crystallographic Meeting [35].

Conflicts of Interest: The authors declare no conflicts of interest. The funders had no role in the design of the study, in the collection, analysis, or interpretation of data, in the writing of the manuscript, or in the decision to publish the results.

References

1. Goodsell, D.S.; Olson, A.J. Structural Symmetry and Protein Function. *Annu. Rev. Biophys. Biomol. Struct.* **2000**, *29*, 105–153. [CrossRef] [PubMed]
2. Rose, P.W.; Prlić, A.; Altunkaya, A.; Bi, C.; Bradley, A.R.; Christie, C.H.; Di Costanzo, L.; Duarte, J.M.; Dutta, S.; Feng, Z.; et al. The RCSB Protein Data Bank: Integrative View of Protein, Gene and 3D Structural Information. *Nucleic Acids Res.* **2017**, *45*, D271–D281. [CrossRef] [PubMed]
3. Burley, S.K.; Berman, H.M.; Kleywegt, G.J.; Markley, J.L.; Nakamura, H.; Velankar, S. Protein Data Bank (PDB): The Single Global Macromolecular Structure Archive. In *Protein Crystallography: Methods in Molecular Biology*; Wlodawer, A., Dauter, Z., Jaskolski, M., Eds.; Humana Press: New York, NY, USA, 2017; Volume 1607, pp. 627–641. ISBN 978-1-4939-6998-2.
4. Marsh, J.A.; Teichmann, S.A. Structure, Dynamics, Assembly, and Evolution of Protein Complexes. *Annu. Rev. Biochem.* **2015**, *84*, 551–575. [CrossRef] [PubMed]
5. Dey, S.; Prilusky, J.; Levy, E.D. QSalignWeb: A Server to Predict and Analyze Protein Quaternary Structure. *Front. Mol. Biosci.* **2022**, *8*, 787510. [CrossRef] [PubMed]
6. Korkmaz, S.; Duarte, J.M.; Prlić, A.; Goksuluk, D.; Zararsiz, G.; Saracbasi, O.; Burley, S.K.; Rose, P.W. Investigation of Protein Quaternary Structure via Stoichiometry and Symmetry Information. *PLoS ONE* **2018**, *13*, e0197176. [CrossRef]
7. Kojić-Prodić, B.; Štefanić, Z. Symmetry versus Asymmetry in the Molecules of Life: Homomeric Protein Assemblies. *Symmetry* **2010**, *2*, 884–906. [CrossRef]
8. Capitani, G.; Duarte, J.M.; Baskaran, K.; Bliven, S.; Somody, J.C. Understanding the Fabric of Protein Crystals: Computational Classification of Biological Interfaces and Crystal Contacts. *Bioinformatics* **2015**, *32*, 481–489. [CrossRef]
9. Dey, S.; Ritchie, D.W.; Levy, E.D. PDB-Wide Identification of Biological Assemblies from Conserved Quaternary Structure Geometry. *Nat. Methods* **2018**, *15*, 67–72. [CrossRef]
10. Krissinel, E.; Henrick, K. Inference of Macromolecular Assemblies from Crystalline State. *J. Mol. Biol.* **2007**, *372*, 774–797. [CrossRef]
11. Ponstingl, H.; Kabir, T.; Thornton, J.M. Automatic Inference of Protein Quaternary Structure from Crystals. *J. Appl. Crystallogr.* **2003**, *36*, 1116–1122. [CrossRef]

12. Bzowska, A.; Kulikowska, E.; Shugar, D. Purine Nucleoside Phosphorylases: Properties, Functions, and Clinical Aspects. *Pharmacol. Ther.* **2000**, *88*, 349–425. [CrossRef] [PubMed]
13. Luić, M.; Štefanić, Z. Can Crystal Symmetry and Packing Influence the Active Site Conformation of Homohexameric Purine Nucleoside Phosphorylases? *Croat. Chem. Acta* **2016**, *89*, 197–202. [CrossRef]
14. Narczyk, M.; Bertoša, B.; Papa, L.; Vuković, V.; Leščić Ašler, I.; Wielgus-Kutrowska, B.; Bzowska, A.; Luić, M.; Štefanić, Z. *Helicobacter pylori* Purine Nucleoside Phosphorylase Shows New Distribution Patterns of Open and Closed Active Site Conformations and Unusual Biochemical Features. *FEBS J.* **2018**, *285*, 1305–1325. [CrossRef] [PubMed]
15. Pugmire, M.J.; Ealick, S.E. Structural Analyses Reveal Two Distinct Families of Nucleoside Phosphorylases. *Biochem. J.* **2002**, *361*, 1–25. [CrossRef] [PubMed]
16. Liu, G.; Cheng, T.; Chu, J.; Li, S.; He, B. Efficient Synthesis of Purine Nucleoside Analogs by a New Trimeric Purine Nucleoside Phosphorylase from Aneurinibacillus Migulanus AM007. *Molecules* **2019**, *25*, 100. [CrossRef]
17. Mikleušević, G.; Štefanić, Z.; Narczyk, M.; Wielgus-Kutrowska, B.; Bzowska, A.; Luić, M. Validation of the Catalytic Mechanism of Escherichia Coli Purine Nucleoside Phosphorylase by Structural and Kinetic Studies. *Biochimie* **2011**, *93*, 1610–1622. [CrossRef]
18. Roszczenko-Jasińska, P.; Wojtyś, M.I.; Jagusztyn-Krynicka, E.K. *Helicobacter pylori* Treatment in the Post-Antibiotics Era—Searching for New Drug Targets. *Appl. Microbiol. Biotechnol.* **2020**, *104*, 9891–9905. [CrossRef]
19. Bubić, A.; Narczyk, M.; Petek, A.; Wojtyś, M.I.; Maksymiuk, W.; Wielgus-Kutrowska, B.; Winiewska-Szajewska, M.; Pavkov-Keller, T.; Bertoša, B.; Štefanić, Z.; et al. The Pursuit of New Alternative Ways to Eradicate *Helicobacter pylori* Continues: Detailed Characterization of Interactions in the Adenylosuccinate Synthetase Active Site. *Int. J. Biol. Macromol.* **2023**, *226*, 37–50. [CrossRef]
20. Mao, C.; Cook, W.J.; Zhou, M.; Koszalka, G.W.; Krenitsky, T.A.; Ealick, S.E. The Crystal Structure of Escherichia Coli Purine Nucleoside Phosphorylase: A Comparison with the Human Enzyme Reveals a Conserved Topology. *Structure* **1997**, *5*, 1373–1383. [CrossRef]
21. Dyzma, A.; Wielgus-Kutrowska, B.; Girstun, A.; Matošević, Z.J.; Staroń, K.; Bertoša, B.; Trylska, J.; Bzowska, A. Trimeric Architecture Ensures the Stability and Biological Activity of the Calf Purine Nucleoside Phosphorylase: In Silico and In Vitro Studies of Monomeric and Trimeric Forms of the Enzyme. *Int. J. Mol. Sci.* **2023**, *24*, 2157. [CrossRef]
22. Bertoša, B.; Mikleušević, G.; Wielgus-Kutrowska, B.; Narczyk, M.; Hajnić, M.; Leščić Ašler, I.; Tomić, S.; Luić, M.; Bzowska, A. Homooligomerization Is Needed for Stability: A Molecular Modelling and Solution Study of Escherichia Coli Purine Nucleoside Phosphorylase. *FEBS J.* **2014**, *281*, 1860–1871. [CrossRef]
23. Wielgus-Kutrowska, B.; Modrak-Wójcik, A.; Dyzma, A.; Breer, K.; Zolkiewski, M.; Bzowska, A. Purine Nucleoside Phosphorylase Activity Decline Is Linked to the Decay of the Trimeric Form of the Enzyme. *Arch. Biochem. Biophys.* **2014**, *549*, 40–48. [CrossRef]
24. Edgar, R.C.; Batzoglou, S. Multiple Sequence Alignment. *Curr. Opin. Struct. Biol.* **2006**, *16*, 368–373. [CrossRef] [PubMed]
25. Krissinel, E. Enhanced Fold Recognition Using Efficient Short Fragment Clustering. *J. Mol. Biochem.* **2012**, *1*, 76–85. [PubMed]
26. Cock, P.J.A.; Antao, T.; Chang, J.T.; Chapman, B.A.; Cox, C.J.; Dalke, A.; Friedberg, I.; Hamelryck, T.; Kauff, F.; Wilczynski, B.; et al. Biopython: Freely Available Python Tools for Computational Molecular Biology and Bioinformatics. *Bioinformatics* **2009**, *25*, 1422–1423. [CrossRef] [PubMed]
27. Bostock, M.; Ogievetsky, V.; Heer, J. D^3 Data-Driven Documents. *IEEE Trans. Vis. Comput. Graph.* **2011**, *17*, 2301–2309. [CrossRef] [PubMed]
28. Shimoyama, Y. pyMSAviz: MSA Visualization Python Package for Sequence Analysis [Computer Software]. 2022. Available online: https://github.com/moshi4/pyMSAviz (accessed on 27 December 2023).
29. Agirre, J.; Atanasova, M.; Bagdonas, H.; Ballard, C.B.; Baslé, A.; Beilsten-Edmands, J.; Borges, R.J.; Brown, D.G.; Burgos-Mármol, J.J.; Berrisford, J.M.; et al. The CCP 4 Suite: Integrative Software for Macromolecular Crystallography. *Acta Crystallogr. D Struct. Biol.* **2023**, *79*, 449–461. [CrossRef]
30. Waskom, M. Seaborn: Statistical Data Visualization. *J. Open Source Softw.* **2021**, *6*, 3021. [CrossRef]
31. Grosse-Kunstleve, R.W.; Sauter, N.K.; Moriarty, N.W.; Adams, P.D. The Computational Crystallography Toolbox: Crystallographic Algorithms in a Reusable Software Framework. *J. Appl. Crystallogr.* **2002**, *35*, 126–136. [CrossRef]
32. Bliven, S.; Lafita, A.; Parker, A.; Capitani, G.; Duarte, J.M. Automated Evaluation of Quaternary Structures from Protein Crystals. *PLoS Comput. Biol.* **2018**, *14*, e1006104. [CrossRef]
33. Schrödinger, LLC. *The PyMOL Molecular Graphics System*, Version 1.8; Schrödinger, LLC: New York, NY, USA, 2015.
34. Xu, Q.; Dunbrack, R.L. Principles and Characteristics of Biological Assemblies in Experimentally Determined Protein Structures. *Curr. Opin. Struct. Biol.* **2019**, *55*, 34–49. [CrossRef] [PubMed]
35. Gomaz, B.; Štefanić, Z. Oligomeric symmetry of purine nucleoside phosphorylases. In Proceedings of the The Twenty-Eighth Croatian-Slovenian Crystallographic Meeting Book of Abstracts, Poreč, Croatia, 7–11 September 2022; Croatian Crystallographic Association: Zagreb, Croatia; p. 35.